ARMA 15-489

The Brittleness Index in Hydraulic Fracturing

Papanastasiou, P.
University of Cyprus, Nicosia, Cyprus
Atkinson, C.
Imperial College London, London, UK

This paper was prepared for presentation at the 49th US Rock Mechanics / Geomechanics Symposium held in San Francisco, CA, USA, 28 June-1 July 2015.

ABSTRACT: We present a new definition of a brittleness index which is used as a criterion for candidate selection of rock intervals for hydraulic fracturing. The new index is a combination of material strength parameters and insitu stresses. It was derived from an analytical model of hydraulic fracturing in weak formations of varying ductility. The model is based on Mohr-Coulomb dislocations that are placed in the effective centres of the complete slip process that is distributed around the crack tip. The new brittleness index varies between 0 and 1 with the one limit to correspond to brittle propagation and the other limit to a fracture that requires infinite energy release per unit advance. The values between 0 and 1 correspond to fracture propagation of increasing ductility from brittle to small scale and finally to large scale yielding. The results are particularly interesting for predicting the propagation of axial fractures in the horizontal direction and their confinement in the vertical direction.

1. INTRODUCTION

The Brittleness index of rocks is often used as a criterion for candidate selection of rock intervals for hydraulic fracturing in shale reservoirs [1]. Several definitions for measuring the brittleness of the rocks were proposed based on different mechanical properties of rocks that are derived from the stress-strain curve or from correlations with physical properties [2, 3, 4]. An inherent problem with some proposed definitions, which are based on simple definitions that were not derived from scientific principles but from correlations that are fitted on dynamic measurements, is that they do not follow the expected trend with some varying parameters such as the confining pressure [1]. Therefore, in unconventional shale reservoirs is important to understand how brittleness can be represented and be used for practical applications of hydraulic fracturing. An extended report and comparisons of 9 different definitions of brittleness numbers based on uniaxial, triaxial and Brazilian tests on gas shale and overburden analogues were presented in [5].

In this work we propose a new definition of a brittleness index which is a combination of material strength parameters and insitu stresses. This definition was derived from an analytical model of hydraulic fracturing in weak formations which accounts for plastic yielding that develops near a hydraulic fracture. The model is based on dislocation theory for Mohr-Coulomb material that accounts for small and large scale plasticity that surrounds the crack tip [6]. The effect of distributed plasticity is replaced by super-dislocations that are placed in the effective centers of the complete slip process that is distributed around the crack tip. The new index varies between 0 and 1 with the one limit to correspond to brittle propagation and the other to a fracture that requires infinite energy release per unit advance. The values between 0 and 1 correspond to fracture propagation of increasing ductility from brittle to small scale and finally to large scale yielding.

The obtained results are useful for the understanding and the modeling of hydraulic fractures in ductile shales. The results are particularly interesting for predicting the propagation of axial fractures in the horizontal direction and their confinement in the vertical direction.

The body of this article is structured as follows: In the next section, we describe briefly the motivation behind this work. In section 3 we describe briefly the Mohr-Coulomb dislocation model for large scale yielding and summarize the dimensionless quantities for the simplified model of the small scale yielding. Results are presented and discussed in section 4 as function of the

brittleness or ductility index. In section 5 we draw the main conclusions.

2. FROM BRITTLENESS TO DUCTILITY

The present work was motivated by the findings of earlier studies for the problem of hydraulic fracturing carried out in order to explain the high-net pressures that are observed in field operations and the discrepancies between simulators and field measurements. This issue was highly debatable in early nineties with different explanation put forward and many studies carried out. Relevant to the topic of this paper are the numerical studies in references [7, 8, 9, 10, 11] which investigated the influence of plastic deformation in hydraulic fracturing using a coupled elastoplastic hydraulic fracturing model based on finite element analysis. It has been shown that plastic yielding near the tip of a propagating fracture provides an effective shielding, resulting in an increase of the rock effective fracture toughness by more than an order of magnitude [9]. The created elasto-plastic fracture is shorter and wider than the elastic fracture of the same volume and hence a higher pressure is needed for propagating an elasto-plastic fracture than an elastic fracture. High net-pressure could also be explained by the underestimation of the minimum insitu-stress from mini-frac tests due to the different closure pattern of elastoplastic fractures [12]. These findings were in agreement with the experimental studies [13].

We recall in particular from [8] results that show the influence of plastic yielding on the apparent fracture toughness increase (Table 1). In those studies the fracture were propagated using robust cohesive interface elements the apparent toughness was determine during propagation using the J-integral [14]. The apparent fracture toughness, called also effective fracture toughness (EFT) was determined once the plastic zones were fully developed.

Table 1.Values of apparent fracture toughness vs stress field and rock strength [9]

σ_3/σ_1	σ_c/σ_T= 60/6	σ_c/σ_T= 20/6	σ_c/σ_T= 20/2
$\frac{\sigma_3}{\sigma_1}=\frac{30}{30}=1$	2.0	2.0	2.0
$\frac{\sigma_3}{\sigma_1}=\frac{45}{30}=1.5$	2.0	4.60	7.31
$\frac{\sigma_3}{\sigma_1}=\frac{60}{30}=2$	2.0	7.03	15.48

The input parameters on which the EFT depends are: the plane strain modulus $E' = (1-\nu^2)$ =31.25GPa, the friction angle and dilation angle, $= \psi = 30^0$, the elastic rock fracture toughness $K_{IC} = 2\ MPa\sqrt{m}$, and the product of pumping parameters viscosity and velocity, $\mu.v = 10^{-8} - 10^{-7}\ MPa\ m$. The varying parameters in the table were the ratio of uniaxial compressive strength over the uniaxial tensile strength, σ_c/σ_T and the ratio of maximum to minimum in-situ stress, σ_3/σ_1.

The main conclusion from Table 1 relevant to this paper is that for the same rock parameters the brittleness or ductility expressed here by the calculated apparent fracture toughness is a strong function of the stress field. Plastic yielding does not take place under a hydrostatic field, even in weak formations (σ_c/σ_T= 20/2). For strong rock formation (σ_c/σ_T= 60/6), plastic yielding does not take place even in a highly non-hydrostatic stress-field. In other words, the brittleness or ductility in hydraulic fracturing is a function of both rock strength and stress field and cannot be considered in isolation of one parameter.

3. MOHR-COULOMB DISLOCATION MODEL

We consider a plane strain pressurized fracture of length 2α which is embedded in a non-isotropic stress field with the minimum compressive stress σ_1 acting in the direction normal to the fracture plane and the maximum compressive stress, σ_3, acting parallel to the crack plane along the propagation direction x (Fig.1). The plastic rock deformation is described by the Mohr-Coulomb model which takes into account the pressure-sensitive behaviour of rocks. A close look at the fracture front of arbitrary shape supports the assumption of plane strain which becomes fully valid for a front with infinity curvature. The fluid pressure acting on the fracture is assumed to be constant, p, although more general loadings can be considered without much difficulty through the stress intensity factor, K_{el}. The constant pressure is a reasonable assumption for a plastic fracture, compared to an elastic fracture, because the former is wider resulting almost in a uniform pressure along the fracture with the pressure drop taking place very near to the fracture tip [8, 9].

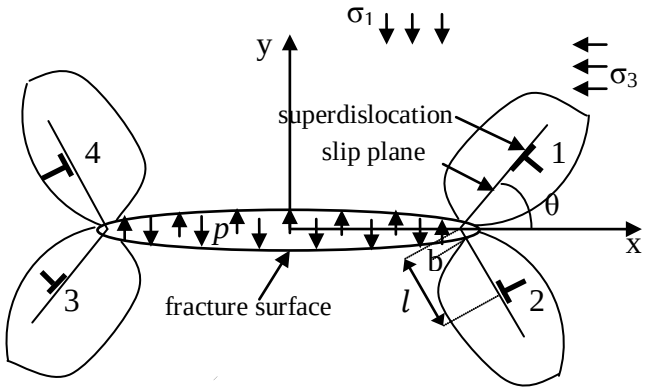

Fig.1. Schematic representation of the dislocation model

The so-called net-pressure is defined by (compressive stresses are negative)

$$\sigma = p + \sigma_1 \tag{1}$$

and is connected with the stress intensity factor for an elastic material via

$$K_{el} = \sigma\sqrt{\pi\alpha} \tag{2}$$

Plastic yielding, whose extent depends on material strength and loading conditions, is expected to take place around the fracture tip due to the high stress concentration. In the dislocation model [5] the plastic zones, which for small scale yielding have the so-called 'rabbit ears' shape, are replaced by a dislocation pair at the center of plastic yielding, $z = a + le^{i\theta}$, where θ is the angle between the crack plane and slip plane and l is the distance from the crack tip along the slip plane (Fig.1).

The unknown positions and strengths of the super-dislocations will be determined from the following three conditions:

- **(i)** the total stress-intensity factor at the crack tip is equal with the material fracture toughness K_{IC} (this can be related to the local energy release at the crack tip so could be set to zero or to a given small value, K_{IC} if required by the model)
- **(ii)** a local equilibrium condition at the dislocation requires the total stresses minus the self stresses of the superdislocation acting at the superdislocation position to be equal to the friction stress due to the Mohr-Coulomb yield criterion
- **(iii)** the total crack opening displacement produced by the model is maximized (this condition assumes the crack will act so as to maximize its opening)

The first condition (i) involves the satisfying of the propagation criterion at the crack-tip given by

$$\sigma\sqrt{\pi\alpha} - \frac{1}{8(\pi\alpha)^{1/2}}\frac{E}{(1-\nu^2)} b\, f = K_{IC} \tag{3}$$

where the first term is due to the external loading whereas the second term gives the contribution of the dislocation internal stress field crack interaction to the stress intensity factor with E and ν being the elastic modulus and Poisson's ratio, respectively, and b denoting the dislocation strength.

The function f is given by [15]

$$f = \frac{8\,\sin\theta}{D}\left[\cos\frac{\theta+\beta}{2} + \frac{l/a}{D^2}\cos\frac{\theta+3\beta}{2} + \frac{(l/a)^2}{D^2}\cos\frac{\theta-3\beta}{2}\right] \tag{4}$$

where

$$\beta = \cos^{-1}\frac{2\left(\frac{l}{\alpha}\right)+\left(\frac{l}{a}\right)^2\cos\theta}{D^2} \tag{5}$$

and

$$D = \frac{l}{\alpha}\left\{1\_4\left(\frac{l}{\alpha}\right)^2\left[1 + \frac{l}{\alpha}\cos\theta\right]\right\}^{1/4} \tag{6}$$

The dislocation strength b is derived from the combination of equations (2), (3) and (4)

$$b = (K_{el} - K_{IC})\, 8\sqrt{\pi\alpha} - \frac{(1-\nu^2)}{E}\frac{1}{f} \tag{7}$$

From the second condition (ii), force equilibrium at the dislocation center is specified in terms of shear stress, τ and normal stress, σ_n which satisfy the Mohr-Coulomb failure criterion where φ and c are the material friction angle and cohesion, respectively.

$$\tau + \sigma_n \tan\varphi = c \tag{8}$$

The shear stress at the dislocation center is given by

$$\tau = \sigma h + \frac{G}{4\pi(1-\nu)} b(g+k) + \frac{(\sigma_1-\sigma_3)}{2}\sin(2\theta) \tag{9}$$

where the first term is due to the crack loading, the second term gives the contribution of the opposite dislocation placed at position $z = a + le^{-i\theta}$, and the last term is due to the original in situ stress field. The functions appearing in (9) are given in [13]

$$h = \sin\theta\left[\cos\theta + \frac{l/\alpha}{D^3}\cos\frac{\theta-3\beta}{2}\right] \tag{10}$$

$$\begin{aligned} g = \frac{2\left(\frac{l}{a}\right)\sin^2\theta}{D^2}\Bigg[& -\frac{3}{2D^2}\cos 2\beta - \frac{2\left(\frac{l}{a}\right)\cos(\theta-2\beta)}{D^2} \\ & -\left(\frac{l/a}{D}\right)^2\cos(2\theta-2\beta) - \frac{\sin(2\beta)}{2\,{}^{l}/_{\alpha}\sin\theta} \\ & + \frac{\sin(\theta-2\beta)}{2\sin\theta} - \frac{\left(\frac{l}{a}\right)\cos(3\beta)}{D^4} \\ & -\left(\frac{l/a}{D^2}\right)^2\cos(\theta-3\beta) - \frac{\sin(\beta)}{2\,\mathrm{D}^2\sin\theta} \\ & - \frac{D^2}{2(l/\alpha)^2}\Bigg] \end{aligned} \tag{11}$$

$$k = -\frac{\cos 2\theta}{a(l/a)} \tag{12}$$

The normal stress σ_n at the dislocation is derived along the same line as

$$\sigma_n = \frac{(K_{el}-K_{IC})}{(2\pi l)^{1/2}}\left[\frac{\cos\theta/\sin\theta + \sin(2\theta) - (3/2)\sin\theta\cos{\theta/_2}^2}{6\sin\theta\cos\left(\frac{\theta}{2}\right)}\right] +$$

$$\frac{K_{el}}{(2\pi l)^{1/2}}\cos\left(\frac{\theta}{2}\right)^3 - \frac{K_{el}}{(\pi\alpha)^{1/2}} + \frac{(\sigma_1+\sigma_3)}{2} + \frac{(\sigma_1-\sigma_3)}{2}\cos(2\theta) \quad (13)$$

The first and second term in (13) were derived under the assumption of the small scale yielding. However, we expect that the biggest contribution to the normal stress σ_n arises from the initial stress field (σ_1, σ_3).

Next, we substitute the last two expressions (9) and (13) for shear stress τ and normal stress, σ_n, respectively, in the Mohr-Coulomb criterion (8) which can be further resolved to provide the dislocation position, l/α. If the normal stress σ_n, is tensile it is not taken into account in the Mohr-Coulomb criterion since it does not provide any frictional resistance to sliding.

Once l is determined the dislocation strength b is calculated from (7). The crack-opening displacement due to the dislocation slip is given by

$$\delta = 2\, b \sin\theta \quad (14)$$

The above equations include as an unknown the angle θ of the slip band on which the superdislocation lies. It is selected in the present model, according to condition (iii) to be that angle which maximizes the crack opening displacement (Fig. 1).

A related quantity of interest is the force on the dislocations. Using the definition of force on a dislocation we get

$$F = 2\, b\, \tau \quad (15)$$

where τ is the finite shear stress (i.e. the total stress minus the self stress of the dislocation). Thus if the whole picture during crack propagation is self-similar F is the energy released per unit advance of the dislocations.

A particularly interesting case is the small scale yielding where the above equations are simplified allowing the determination of the important parameters. Small scale yielding was studied in reference [1] assuming, $l \ll \alpha$ and large scale yielding in [16]. Though the material fracture toughness was introduced in this study, in the next expressions and comparisons we will assume that is zero, $K_{IC} = 0$. In this case the functions *f, h, g, k* are much simplified allowing a closed form solution for the dislocation length l.

We summarize bellow these results in dimensionless forms that provide a convenient way for discussing particular cases and comparison with the results of large scale yielding.

The dislocation position, l, the dislocation strength, b, the crack opening displacement, δ, and the dislocation force, F, are given by the following equations

$$\frac{l^{1/2}}{K_{el}/c} = \left(\frac{2}{\pi}\right)^{1/2} \frac{f_1(\theta)+\tan\varphi f_2(\theta)}{f_0} \quad (16)$$

$$\frac{b}{(1-\nu^2)K_{el}^2/(Ec)} = \frac{4}{3}\frac{f_1(\theta)/f_3(\theta)+\tan\varphi f_2(\theta)/f_3(\theta)}{f_0} \quad (17)$$

$$\frac{\delta}{(1-\nu^2)K_{el}^2/(Ec)} = \frac{8}{3}\frac{f_1(\theta)/f_4(\theta)+\tan\varphi f_2(\theta)/f_4(\theta)}{f_0} \quad (18)$$

$$\frac{F}{(1-\nu^2)K_{el}^2/(Ec)} = \frac{8}{3}\frac{1}{f_3(\theta)}\left\{\left[\frac{f_1(\theta)+\tan\varphi f_2(\theta)}{f_0}\right]\left[f_0 + \frac{(\sigma_3-\sigma_1)}{2c}\sin(2\theta)\right] - \tan\varphi\, f_2(\theta)\right\} \quad (19)$$

$$f_0\left(\frac{(\sigma_3-\sigma_1)}{2c}, \frac{p}{c}, \varphi, \theta\right) = \left[1 - \frac{(\sigma_3-\sigma_1)}{2c}\sin(2\theta)\right] + \tan\varphi\left[\frac{p}{c} + \frac{(\sigma_3-\sigma_1)}{2c}(1-\cos(2\theta))\right] \quad (20)$$

$$f_1(\theta) = \frac{2\sin^2\theta\cos^2\left(\frac{\theta}{2}\right)-1}{12\sin\theta\cos\left(\frac{\theta}{2}\right)} \quad (21)$$

$$f_2(\theta) = \frac{\cos\theta/\sin\theta + \sin(2\theta) - 1.5\,\sin\theta\,\cos^2\left(\frac{\theta}{2}\right)}{12\sin\theta\cos\left(\frac{\theta}{2}\right)} + \frac{\cos^3\left(\frac{\theta}{2}\right)}{2} \quad (22)$$

$$f_3(\theta) = \sin\theta\cos\left(\frac{\theta}{2}\right) \quad (23)$$

$$f_4(\theta) = \cos\left(\frac{\theta}{2}\right) \quad (24)$$

The quantities $f_1(\theta)\ to\ f_4(\theta)$ in Eqs (21)-(25) are functions only of the inclination of the superdislocation angle θ that maximizes the crack opening displacement. The loading conditions and the strength of the rock enter into the problem only through the function f_0 in Eq.(20). A careful consideration of Eq.(20) reveals that both the insitu stresses and the rock strength can be combined to a dominant single parameter

$$t = \frac{(\sigma_1-\sigma_3)}{2c\cos\varphi - (\sigma_1+\sigma_3)\sin\varphi} \quad (25)$$

which will be used to identify the brittleness index in hydraulic fracturing supported by the results of the next section.

4. RESULTS

A series of parametric studies has been carried out for particular cases to show that the Mohr-Coulomb

dislocation model can capture the essential dependence of the crack-tip plasticity on the important parameter of Eq. (25). We compare the same results with those obtained under the assumption of the small scale yielding. We plotted the results using the dimensionless quantities which were derived for the small scale yielding assumption. Figures 2 and 3 show the calculated dimensionless center of dislocation, $l^{1/2}/[K_{el}/c]$, the strength of the dislocation, $b/[(1-\nu^2)K_{el}^2/(Ec)]$, the crack opening displacement, $\delta/[(1-\nu^2)K_{el}^2/(Ec)]$ and the dislocation force, $F/[(1-\nu^2)K_{el}^2/(Ec)]$ for varying loading conditions and material parameters expressed through the single parameter of Eq.(25) . These values were calculated for the value of angle θ that maximizes the crack opening displacement, δ. The corresponding critical value of θ is also shown in these figures and appears to be identical for both small scale yielding and large scale yielding. In both Figs 2 and 3 the results of the small scale yielding are shown by the solid lines and the large scale yielding with the dashed lines.

4.1. Frictionless material

Figure 2 shows the results for a frictionless material or equivalently to undrained conditions which will be valid in the case of hydraulic fracturing in very low permeability reservoirs such as the gas-shale and oil-shale reservoirs. The dimensionless quantities (16)-(19) depend only on the loading parameter

$$t = \frac{(\sigma_1-\sigma_3)}{2c_u} \qquad (26)$$

where c_u is the undrained cohesion of the material.

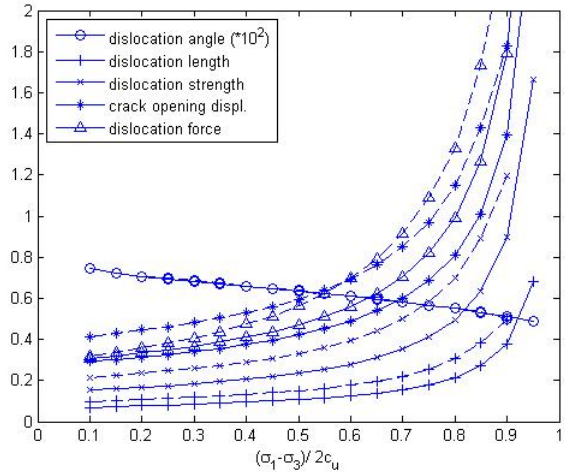

Fig. 2. Dimensionless quantities vs ductility number for undrained material.

The parameter of Eq. (26) in general, dictates the scale of plastic yielding for a von Mises material. This parameter can take values between 0 and 1. For 0 value the material is elastic or brittle during fracturing. For increasing value the scale of plastic yielding increases. The limit value of this parameter is *1* in which case the material will yield everywhere requiring infinite energy for fracturing.

4.2. Frictional material

Figure 3 shows the results for a frictional material or equivalently for drained conditions which will be valid in slow hydraulic fracturing operations in permeable materials such as sandstones. In this case the dominant parameter *t* takes the full expression of Eq.(25) varying between 0 and 1 with the value *0* to correspond to brittle propagation and *1* to a fracture that requires infinite energy release per unit advance. The values between 0 and 1 correspond to fracture propagation of increasing ductility from brittle to small scale and finally to large scale yielding. We see that all the quantities (other than the dislocation angle) obtained from the large scale yielding model are greater than those calculated under the assumption of the small scale yielding. For very small values of the applied load the two models give relatively close results, as expected, because in that range the dislocation length is small compared to the fracture length (Figs 2, 3). The calculated quantities increase abruptly when $t \to 1$ indicating large scale yielding. In this region we see significant deviation of the large scale yielding results (dashed lines) from the results of the small scale yielding (solid lines) which were obtained under the assumption of $l \ll \alpha$.

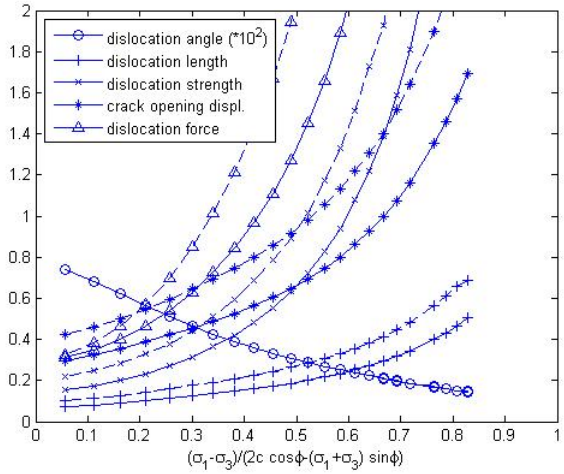

Fig. 3. Dimensionless quantities vs ductility number for frictional material.

In both Figs 2 and 3 the results at the RHS of the curves are interpreted to correspond to a fracture front that propagates vertically where as the results of LHS correspond more to a fracture front that propagates horizontally. It is clear that much higher energy is

needed for a fracture to propagate vertically. For example in undrained conditions (Fig.2) a fracture with $t = 0.9$ to propagate vertically will require 7 times more energy than propagating horizontally which may correspond to $t = 0$. In drained condition (Fig.3) for $t = 0.5$ the fracture will require more than 10 times the energy that will require for propagating horizontally in isotropic stress field, $t = 0$.

These results are particularly interesting for hydraulic fracturing in gas-shale and oil-shale formations in addressing the risk of contamination of water resources in upper layers by hydraulic fractures that may propagate into those layers. This finding supports the argument that a hydraulic fracture will propagate horizontally with high probability of remaining contained in the pay zone.

The different definitions proposed for the brittleness index vary between 0 and 1 [1, 2, 3, 4, 5] but with the limit of *1* to express brittle behaviour and the limit of *0* to express the full ductile behavior. The present definition of Eqs (25) and (26) which express the degree of ductility vary also between 0 and 1 but with the limits to express the opposite deformation behavior. In order to be consistent with the other definitions [1, 2, 3, 4, 5], the brittleness index of this study can be defined as

$$B = 1 - t = 1 - \frac{(\sigma_1 - \sigma_3)}{2c\cos\varphi - (\sigma_1 + \sigma_3)\sin\varphi} \qquad (27)$$

We recognize that for practical applications the Oil industry would prefer quantities that are routinely measured in the field such as the dynamic young's modulus determined from sonic data. The proposed definitions (25)-(26) will require the knowledge of the vertical and horizontal stresses and the strength of the rock which can obtained from correlation functions with the dynamic measurements [17]. The vertical insitu stress is determined from integrating the density logs and the horizontal stress from mini-frac test masurements.

5. CONCLUSIONS

We introduced a new brittleness index, Eq. (27) which can be used as a criterion for candidate selection of rock intervals for hydrulic fracturing in shale reservoirs. The index was derived from a Mohr-Coulomb dislocation model that accounts for small and large scale plasticity that surrounds the hydraulic fracture tip. The new index is a combination of the insitu stresses and the rock strength parameters. It varies between 0 and 1 with the one limit to correspond to brittle propagation and the other limit to a fracture that requires infinite energy release per unit advance. The values between the two limits correspond to fracture propagation of varying ductility from brittle to small scale and finally to large scale yielding. The findings are consistent with the results of earlier studies based on coupled elastoplastic hydraulic fracturing finite element analysis. The results predict that fracture propagation in the horizontal direction is more likely to take place in the brittle regime where as in the vertical direction in the ductile regime promoting fracture containment in the vertical direction.

6. REFERENCES

1. Rickman, R., Mullen, M., Petre, E., Grieser, B., Kundert, D., 2008. A practical use of shale petrophysics for stimulation design optimization: All shale plays are not clones of the Barnett shale. *SPE 115258; Proc. Ann. Tech. Conf., Denver, Co., USA, 21-24 September 2008*. 11 pp.

2. Hucka, V., Das, B., 1974. Brittleness determination of rocks by different methods. *Int. J. Rock Mech. Min. Sci. & Geomech. Abstr*. 11, 389-92

3. Holt, R.M., Fjær, E., Nes, O.-M., Alassi, H.T., 2011. A shaly look at brittleness. *ARMA 11-366; 10 pp.*

4. Yang, Y., Hiroki, S., Hows, A., Zoback, M.D. 2013. Comparison of brittleness indices in organic-rich shale formations. *ARMA 13-403.* 7 pp

5. Holt, R.M., Fjær, E., Stenebraten J.F., Nes, O.-M. 2015. Brittleness of Shales: Relevance to borehole collabse and hydraulic fracturing. *J. Petroleum Sciences and Engineering.* (submitted).

6. Papanastasiou, P. Atkinson, C. (2000). Representation of crack-tip plasticity in pressure sensitive geomaterials. *Int. J. Fracture*, 102, 271-286.

7. Papanastasiou, P. and Thiercelin, M. 1993. Influence of inelastic rock behaviour in hydraulic fracturing. *Int. J. Rock Mechanics and Mining Sciences*, 30, No.7, 1241-1247.

8. Papanastasiou, P. 1997. The influence of plasticity in hydraulic fracturing. *Int. J. Fracture*, 84, 61-79.

9. Papanastasiou, P. 1999. The effective fracture toughness in hydraulic fracturing. *Int. J. Fracture*, 96, 127-147.

10. Alassi, H.T., Holt, R., Nes, O-M., Pradhan, S., 2011. Realistic geomechanical modeling of hydraulic fracturing in fractured reservoir rock. *CSUG/SPE 149375.* 6 pp.

11. Sarris, E., Papanastasiou, P., 2013. Numerical Modelling of Fluid-Driven Fractures in Cohesive Poro-elastoplastic Continuum, *Int. J. Numer. Anal. Meth. Geomech*, v. 37 (12), 1822-1846.

12. Papanastasiou P. 2000. Hydraulic fracture closure in pressure-sensitive elastoplastic medium. *Int. J. Fracture*, 103, pp.149-161.

13. van Dam D.B., Papanastasiou P, de Pater C.J. 2002. Impact of rock plasticity on hydraulic fracture

propagation and closure. *J. SPE Production & Facilities*, 17 (3), 149-159.

14. Rice, J.R. (1968). A path-independent integral and the approximate analysis of strain concentration by notches and cracks. *J. Applied Mechanics Transition ASME*, 35, 379–386.

15. Atkinson, C. and Kanninen, M.F. (1977). A simple representation of crack tip plasticity: The inclined strip-yield superdislocation model. *Int. J. Fracture*, 13, 151-163.

16. Papanastasiou P. and Atkinson C. 2006. Representation of crack-tip plasticity in pressure-sensitive geomaterials: Large scale yielding, *Int. J. Fracture*, 139, 137-144.

17. Plumb, R. A., 1994. Influence of composition and texture on the failure properties of clastic rocks. SPE/ISRM 28022; *In Proc. EUROCK'94 Rock Mechanics in Petroleum Engineering.* A.A.Balkema, 13-20.